Localized electromagnetic waves in a layered periodic dielectric medium with a defect

Alexander Figotin and Vladimir Gorentsveig
Department of Mathematics, University of North Carolina at Charlotte, Charlotte, North Carolina 28223
(Received 12 January 1998)

Electromagnetic waves propagating perpendicularly to the layers in a layered periodic dielectric medium with an embedded defect are studied. We develop an analytical method to obtain the solution to the spectral problem for such a one-dimensional system with an arbitrary configuration of the period cell and of the defect. It is shown that the defect induces localized electromagnetic modes with a discrete spectrum of frequencies located in the band gaps of an unchanged continuous spectrum. We derive equations for the gaps, for the discrete spectrum, and for the localization rate. For a case of a two-layer periodic medium with an embedded one-layer defect we carry out a complete analysis of the dependence of the frequency and of the rate of localization of a defect-induced mode on the parameters of the defect and of the periodic medium. [S0163-1829(98)03925-3]

I. INTRODUCTION

Periodic dielectric media (called photonic crystals) exhibiting band gaps in the frequency spectrum have attracted significant attention in recent years.[1–5] The problem of localized electromagnetic waves with frequencies arising in the gaps due to an isolated defect in the periodic structure is of special interest.[6,7] Such modes were observed experimentally for microwaves in a three-dimensional (3D) system,[8] for 2D systems,[9–11] and for a 1D system.[9] The problem was addressed theoretically for 3D systems[8,12] using a supercell method with plane-wave expansion and for 2D systems[13,9] using the Green's function method. Although localized states with frequencies in a gap were obtained, the convergence of the numerical computations is slow.[14,9,15]

The simplest system exhibiting localized electromagnetic modes is a layered periodic medium with an embedded defect layer and with electromagnetic waves polarized parallel to the layers. Such a 1D system allows us to analyze the conditions for the rise of a localized mode in a gap and the dependence of its frequency and of the localization rate on the parameters of the system. The results for the layered systems could give some important analytical insight for further numerical investigation of 2D and 3D systems. They are also useful for a variety of applications such as microwave filters, lasers, and light-emitting diodes.[2,4,5]

The 1D problem has been considered for the simplest case of a vacancy defect[9] and for a case of a substitution defect[15] in a two-layer periodic medium. Both papers offered analytical solutions for the defect modes using the transfer-matrix method and the symmetry of inversion for these special configurations.

In this paper we study 1D systems using a different method, which we call the propagation matrix method. The method is a generalization of the monodromy matrix approach to the spectral problem for pure periodic 1D Schrödinger[16] and Maxwell[17] operators. It enables us to obtain analytically a solution to the spectral problem for a 1D system with any configuration of a defect embedded in an arbitrary periodic medium. If the Cauchy problem for the wave equation is solved on a one period cell interval and on the defect interval, then the spectral problem reduces to a matrix recurrence equation on a chain of the cell boundary points spaced with one period.

We show that a defect embedded in the periodic medium does not alter its continuous spectrum which exhibits frequency bands separated by gaps and corresponds to propagating waves. The defect induces a discrete set of frequencies which are located in the gaps of the continuous spectrum and correspond to localized modes that decay exponentially away from the defect. We derive the equations for the band gaps and for the frequencies of localized modes and an explicit formula for the localization rate. All the equations are written in terms of the frequency-dependent propagation matrices for the periodic medium and for the defect. We show that the rate of localization of a defect-induced mode depends on the configuration of the defect only through the frequency of the mode and that the wave delocalizes when its frequency approaches the gap edges.

We apply the method to the simplest situation of a one-layer defect in a two-layer periodic medium where we obtain explicit formulas for entries of the propagation matrices. Using the phase-amplitude representation[18] for the gap-edge equation we show the following: (i) the gap width oscillates with the gap number while an average gap width does not decrease for higher gaps; (ii) the gap-edge values decrease while the width of each gap oscillates with the increase of the dielectric contrast or of the thickness ratio for the two-layer medium; (iii) the ratio of an average gap width over an average bandwidth increases with the increase of the dielectric contrast.

As to the localized modes, we prove analytically that there is always at least one such state in each gap for the one-layer defect. We also show that (i) the rate of localization is maximal when the mode frequency is in the middle of the gap; (ii) the rate maximum is greater for wider gaps; (iii) the upper limit for the localization rate depends only on the dielectric contrast between two layers in the period cell and increases with the contrast. In addition to that we observe that when the dielectric contrast between the defect and the medium or relative thickness of the defect layer increases, then: (i) localized mode frequencies arise at the upper edge

of a gap and vanish at the lower edge of the gap, while in between, the frequency of each such mode decreases monotonically; (ii) an average number of the localized states in each gap increases.

II. BASIC EQUATIONS

We consider a layered lossless dielectric medium and electromagnetic waves propagating perpendicularly and, hence, polarized parallel to the layers. For such a system the Maxwell equations reduce to the following scalar wave equation for the magnetic field $H(x,t)$:

$$c^{-2}\partial_t^2 H = \partial_x \frac{1}{\varepsilon(x)} \partial_x H, \tag{1}$$

where x is the coordinate along the direction orthogonal to the layers, c is the speed of light in the vacuum, and $\varepsilon(x) \geqslant 1$ is the position-dependent dielectric permittivity.

Considering time harmonic fields,

$$H(x,t) = \psi(x)\exp(i\omega t) + \text{c.c.}, \tag{2}$$

we arrive at the following spectral problem for the spatial modes:

$$-\partial_x \frac{1}{\varepsilon(x)} \partial_x \psi(x) = \left(\frac{\omega}{c}\right)^2 \psi(x), \tag{3}$$

where $\psi(x)$ is supposed to be bounded everywhere:

$$|\psi(x)| < \infty. \tag{4}$$

We study an infinite layered periodic medium of a period L with an embedded defect of a finite thickness D. In terms of the dielectric function $\varepsilon(x)$ we have

$$\begin{gathered} \varepsilon(D+mL+x') = \varepsilon_1(x'), \quad m = 0,1,2,\ldots, \\ \varepsilon(mL+x') = \varepsilon_1(x'), \quad m = -1,-2,-3,\ldots \\ \text{at } \ 0 < x' < L, \\ \varepsilon(x) \quad \text{is arbitrary at } \ 0 < x < D, \end{gathered} \tag{5}$$

i.e., the same period cell, $\varepsilon_1(x')$ $(0<x'<L)$ of the thickness L repeats on the right and on the left of the defect interval $0<x<D$.

The simplest realization of such a system is a periodic medium with two homogeneous layers of different substances in the period cell,

$$\begin{gathered} \varepsilon_1(x') = \epsilon_1, \quad 0 < x' < L_1, \\ \varepsilon_1(x') = \epsilon_2, \quad L_1 < x' < L_1 + L_2 = L, \end{gathered} \tag{6}$$

and with one homogeneous layer of a third substance as the defect,

$$\varepsilon(x) = \epsilon_3, \quad 0 < x < D. \tag{7}$$

Note that Eq. (3) can be scaled as follows:

$$x \to \tilde{x} = x/L_0, \quad \varepsilon \to \tilde{\varepsilon} = \varepsilon/\epsilon_0, \quad \omega \to \tilde{\omega} = \omega L_0 \sqrt{\epsilon_0}. \tag{8}$$

Hence, the frequency spectrum depends, up to a certain factor, only on the relative values of the dielectric permittivity as a function of the relative coordinate. For a system of homogeneous layers, as in Eq. (6), the thickness and dielectric constant for one of the layers can be taken as the scaling parameters L_0 and ϵ_0.

III. PROPAGATION MATRIX METHOD FOR THE SPECTRAL PROBLEM

Let us introduce a sequence $\{x_n\}$ of points spaced with the one-cell interval in the two halves of the periodic medium starting on both sides of the defect,

$$\begin{gathered} x_n = D + (n-1)L, \quad n = 1,2,3,\ldots, \\ x_n = (n+1)L, \quad n = -1,-2,-3,\ldots . \end{gathered} \tag{9}$$

We will call the points x_n the cell boundary points.

Each solution $\psi(x)$ of the second-order equation (3) on an interval (x_0, x_0+l) is uniquely defined by initial values of the function and its derivative, $\psi(x_0)$ and $\psi'(x_0)$, and can be expressed as their linear combination with functional coefficients based on a pair of fundamental solutions, $f_1(x)$ and $f_2(x)$. If we introduce the two-component column vector

$$\Psi(x) = \begin{bmatrix} \psi(x) \\ \psi'(x)/\varepsilon(x) \end{bmatrix}, \tag{10}$$

then we can write the propagation relation,

$$\Psi(x) = \mathbf{P}(x, x_0; \omega)\Psi(x_0), \quad x > x_0, \tag{11}$$

where $\mathbf{P}(x,x_0;\omega)$ is the 2×2 frequency-dependent matrix of propagation of the vector $\Psi(x)$ over the subinterval (x_0,x):

$$\mathbf{P}(x,x_0) = \mathbf{Q}(x)\mathbf{Q}^{-1}(x_0), \tag{12}$$

$$\mathbf{Q}(x) = \begin{bmatrix} f_1(x) & f_2(x) \\ f_1'(x)/\varepsilon(x) & f_2'(x)/\varepsilon(x) \end{bmatrix}. \tag{13}$$

We prefer to consider $\psi'(x)/\varepsilon(x)$ [rather than just $\psi'(x)$] as the second component of $\Psi(x)$ in Eq. (10) because it is still continuous [see Eqs. (3), (4)] when the dielectric function $\varepsilon(x)$ is only piecewise continuous [as in Eqs. (6), (7)]. Due to that, the matrix of propagation over an interval divided into subintervals is equal to just the product of matrices of propagation over the subintervals:

$$\mathbf{P}(x,x_0) = \mathbf{P}(x,x')\mathbf{P}(x',x_0), \quad x_0 < x' < x. \tag{14}$$

In addition, the matrix $\mathbf{P}(x'',x';\omega)$ of propagation for vector $\Psi(x)$ in Eq. (10) on any subinterval (x',x'') is unimodular [see Eq. (12)]:

$$\det[\mathbf{P}(x'',x';\omega)] = 1 \tag{15}$$

because $\partial_x \det[\mathbf{Q}(x)] \equiv 0$ according to Eqs. (10) and (3). Note also that since the coefficients in Eq. (3) are real the entries of the matrix $\mathbf{P}(x,x_0;\omega)$ are real valued.

Considering the propagation relation (11) for a one-period cell interval, (x_n, x_{n+1}), $n = 1, \pm 2, \pm 3, \ldots$, we find that the values of the vector function $\Psi(x)$ at two subsequent cell boundary points on the same side of the defect are related as follows:

$$\Psi(x_{n+1})=\mathbf{T}(\omega)\Psi(x_n),\quad n=1,\pm 2,\pm 3,\ldots, \tag{16}$$

$$\mathbf{T}(\omega)=\begin{bmatrix} t_{11}(\omega) & t_{12}(\omega)\\ t_{21}(\omega) & t_{22}(\omega)\end{bmatrix}=\mathbf{P}(x_{n+1},x_n;\omega), \tag{17}$$

where $\mathbf{T}(\omega)$ is the matrix of propagation over one period cell. Due to translational symmetry (5) of Eq. (3) within the periodic medium, the matrix $\mathbf{T}(\omega)$ does not depend on the index n of the cell boundary point x_n.

Applying the propagation relation (11) to the defect interval (x_{-1},x_1) we obtain the relation between the values of the vector function $\Psi(x)$ at the cell boundary points $x_{-1}=0$ and $x_1=D$ at the edges of the defect:

$$\Psi(x_1)=\mathbf{S}(\omega)\Psi(x_{-1}), \tag{18}$$

$$\mathbf{S}(\omega)=\begin{bmatrix} s_{11}(\omega) & s_{12}(\omega)\\ s_{21}(\omega) & s_{22}(\omega)\end{bmatrix}=\mathbf{P}(x_1,x_{-1};\omega), \tag{19}$$

where $\mathbf{S}(\omega)$ is the matrix of propagation over the defect interval.

To actually find the matrices $\mathbf{T}(\omega)$ and $\mathbf{S}(\omega)$ one has to solve Cauchy problem for Eq. (3) on the one-cell interval and on the defect interval, respectively. Then the spectral problem (3), (4) reduces to solving the recurrence equation (16) on each side of the defect, together with the relation (18) over the defect, for $\Psi(x_n)$ as a function of the cell boundary point number, $n=\pm 1,\pm 2,\pm 3,\ldots$. The frequency spectrum is found as all values ω for which the solution is bounded,

$$|\Psi(x_n)|<\infty \quad \text{at } |n|\to\infty. \tag{20}$$

Let us represent the vector $\Psi(x_n)$ as a linear combination

$$\Psi(x_n)=\sum_{i=1,2} c_i(x_n)U_i, \tag{21}$$

where U_i, $i=1,2$, are the eigenvectors of the matrix $\mathbf{T}(\omega)$ corresponding to its eigenvalues τ_i, $i=1,2$, i.e.,

$$\mathbf{T}(\omega)U_i=\tau_i U_i. \tag{22}$$

We readily find the eigenvectors in terms of the entries of the matrix $\mathbf{T}(\omega)$:

$$U_i=\begin{bmatrix} t_{12}\\ \tau_i-t_{11}\end{bmatrix}\quad (i=1,2) \tag{23}$$

(we have specified an arbitrary factor taking it equal to 1).

Because all entries of the matrix $\mathbf{T}(\omega)$ are real valued its two eigenvalues are either complex conjugate or both real. Since the matrix $\mathbf{T}(\omega)$ is unimodular [see Eqs. (17) and (15)], its two eigenvalues are mutually inverse:

$$\tau_1\tau_2=1. \tag{24}$$

Note that for the trace of the matrix $\mathbf{T}(\omega)$ we have

$$\mathrm{Tr}[\mathbf{T}(\omega)]=\tau_1+\tau_2=\tau_1+\frac{1}{\tau_1}. \tag{25}$$

Applying recurrence (16) (or its inverse) repeatedly, starting at $n=1$ (or at $n=-1$) with $\Psi(x_{\pm 1})$ decomposed as in Eq. (21), and using Eq. (22), we obtain the general solution for $\Psi(x_n)$:

$$\begin{aligned}\Psi(x_n)&=\sum_{i=1,2} c_i^{+}\tau_i^{n-1}U_i,\quad n=1,2,3,\ldots .\\ \Psi(x_n)&=\sum_{i=1,2} c_i^{-}\tau_i^{n+1}U_i,\quad n=-1,-2,-3,\ldots,\end{aligned} \tag{26}$$

where

$$c_i^{\pm}=c_i(x_{\pm 1}),\quad i=1,2. \tag{27}$$

Because of relation (24) between eigenvalues τ_1 and τ_2 there are two possible situations for their absolute values. The first one is

$$|\tau_1|=|\tau_2|=1. \tag{28}$$

All different pairs of the eigenvalues satisfying Eqs. (28) and (24) can be represented as

$$\tau_1=e^{ik},\quad \tau_2=e^{-ik},\quad 0\leqslant k\leqslant\pi \tag{29}$$

(note that such eigenvalues are complex conjugate).

In this case, the sequence $\Psi(x_n)$ defined by Eq. (26) will just oscillate as $n\to\pm\infty$. Hence, the boundedness condition (20) is satisfied for any coefficients $c_i^{\pm}$. The vector equation (18) due to the defect relates the two pairs of coefficients, c_i^{+} and c_i^{-}, $i=1,2$, so just one of the pairs remains arbitrary. Using Eqs. (29) and (25) we obtain the equation

$$\mathrm{Tr}[\mathbf{T}(\omega)]=2\cos(k),\quad 0\leqslant k\leqslant\pi, \tag{30}$$

which determines the dispersion relation $\omega=\omega(k)$. This continuous spectrum of ω coincides with the entire spectrum for the periodic media with no defect.[16] In general, it exhibits bands of allowed values of ω, separated by gaps described with the inequality following from Eq. (30),

$$|\mathrm{Tr}[\mathbf{T}(\omega)]|>2. \tag{31}$$

The second situation is

$$|\tau_1|>1,\quad |\tau_2|<1 \tag{32}$$

(note that in this case the eigenvalues must be real). Then the boundedness condition (20) is satisfied only if

$$c_1^{+}=0,\quad c_2^{-}=0, \tag{33}$$

and $\Psi(x_n)$ in Eq. (26) is a multiple of only one of the two eigenvectors on each side of the defect:

$$\begin{aligned}\Psi(x_n)&=c_2^{+}\tau_2^{n-1}U_2,\quad n=1,2,3,\ldots,\\ \Psi(x_n)&=c_1^{-}\tau_1^{n+1}U_1,\quad n=-1,-2,-3,\ldots .\end{aligned} \tag{34}$$

This means that $\Psi(x_n)$ decays exponentially at $n\to\pm\infty$ on both sides of the defect [see Eq. (24)],

$$\begin{aligned}\Psi(x_n)&=C^{\pm}\tau_1^{-(|n|-1)},\quad n=\pm 1,\pm 2,\pm 3,\ldots,\\ C^{+}&=c_2^{+}U_2,\quad C^{-}=c_1^{-}U_1,\end{aligned} \tag{35}$$

with the multiplicative rate of the localization equal to

$$\tau = |\tau_1|. \tag{36}$$

An effective localization length can be defined as

$$\lambda = L/\ln(\tau). \tag{37}$$

Relation (18) due to the defect gives a homogeneous system of two equations,

$$c_2^+ U_2 = c_1^- \mathbf{S}(\omega) U_1 \tag{38}$$

that relates two coefficients, c_2^+ and c_1^-, so one of them can be chosen arbitrarily and then the other one has to be found from Eq. (38). The solvability condition,

$$\frac{(U_2)_2}{(U_2)_1} = \frac{(\mathbf{S}(\omega)U_1)_2}{(\mathbf{S}(\omega)U_1)_1}, \tag{39}$$

where $(\cdot)_1$ and $(\cdot)_2$ stand for the first and the second components of a column vector, relates the frequency ω and the localization factor τ_1. Indeed, due to Eqs. (23) and (24), relation (39) takes the form

$$\frac{\tau_1^{-1} - t_{11}}{t_{12}} = \frac{s_{21}t_{12} + s_{22}(\tau_1 - t_{11})}{s_{11}t_{12} + s_{12}(\tau_1 - t_{11})}, \tag{40}$$

where the entries t_{ij} and s_{ij} are functions of the frequency ω.

Equation (25) gives the second relation between τ_1 and ω which can be written in terms of the entries of the matrix $\mathbf{T}(\omega)$ as follows:

$$t_{11} + t_{22} = \tau_1 + \tau_1^{-1}. \tag{41}$$

The system of equations (40) and (41) determines possible values of the frequency ω for localized states (35) induced by the defect and the corresponding values of the localization factor τ_1. Because the absolute value of the right-hand side in Eq. (41) exceeds 2 for any real-valued τ_1 these values of ω should be located in the gaps (31) of the continuous spectrum.

With a proper substitution of τ_1^{-1} from Eq. (41) and use of the unimodularity of the matrix $\mathbf{T}(\omega)$,

$$t_{11}t_{22} - t_{12}t_{21} = 1 \tag{42}$$

[see Eqs. (17) and (15)], we obtain from Eq. (40) the following relation:

$$\tau_1 = \frac{s_{11}t_{22} + s_{22}t_{11} - s_{12}t_{21} - s_{21}t_{12}}{s_{11} + s_{22}}. \tag{43}$$

Excluding τ_1 from the system of equations (41) and (43) we obtain the following equation for values of ω for the localized states:

$$\chi^2 + 1 = \eta^2, \tag{44}$$

where

$$\chi(\omega) = -\frac{(s_{11} - s_{22})(t_{11} - t_{22}) + 2(s_{12}t_{21} + s_{21}t_{12})}{2(s_{11} + s_{22})} \tag{45}$$

and

$$\eta(\omega) = (t_{11} + t_{22})/2, \tag{46}$$

with an additional condition

$$\mathrm{sgn}\,(\chi) = \mathrm{sgn}\,(\eta), \tag{47}$$

which follows from the inequality

$$|\tau_1| = |\eta + \chi| \geq |\tau_1^{-1}| = |\eta - \chi|. \tag{48}$$

We can combine Eq. (44) with condition (47) as follows:

$$\mathrm{sgn}\,(\chi)\sqrt{\chi^2 + 1} = \eta. \tag{49}$$

Solutions of Eq. (49) form the discrete spectrum of ω induced by the defect embedded into the periodic medium.

The localization factor τ_1 as a function of ω can be easily found from Eq. (41):

$$\tau_1 = \eta + \mathrm{sgn}\,(\eta)\sqrt{\eta^2 - 1}. \tag{50}$$

We see in Eqs. (50), (46) that the function $\tau_1(\omega)$ depends on the configuration of the defect only through the frequency ω. Note also that the inequality (31) for the gaps between bands of the continuous spectrum of ω can be written as

$$|\eta(\omega)| > 1. \tag{51}$$

According to Eqs. (50) and (51), the localization rate τ Eq. (36) decreases to 1 (the wave delocalizes) when the frequency ω for the localized state approaches the gap edges.

IV. TWO-LAYER CELL PERIODIC MEDIUM WITH ONE-LAYER DEFECT

We apply the propagation matrix method to the periodic medium with two layers in the period cell (6) with one-layer defect (7). Within a homogeneous layer $x_l < x < x_l + h$ with constant dielectric permittivity $\varepsilon(x) = \epsilon$ Eq. (3) simplifies as follows:

$$-\partial_x^2 \psi(x) = (\alpha\nu)^2 \psi(x), \tag{52}$$

$$\alpha = \sqrt{\epsilon}, \quad \nu = \omega/c. \tag{53}$$

Given the initial values $\psi(x_l)$ and $\psi'(x_l)$ at the left end point x_l of the layer interval, we can write the solution of Eq. (52) as

$$\psi(x) = \psi(x_l)\,\cos\,(\alpha\nu(x - x_l)) + \frac{\psi'(x_l)}{\alpha\nu}\,\sin\,(\alpha\nu(x - x_l)). \tag{54}$$

Hence, the matrix of propagation (11) for $\Psi(x)$ Eq. (10) in the homogeneous layer is

$$\mathbf{P}(x, x_l; \omega) = \mathbf{R}(x - x_l; \alpha; \omega), \quad x_l < x < x_l + h, \tag{55}$$

$$\mathbf{R}(y; \alpha; \omega) = \begin{bmatrix} \cos\,(\alpha\nu y) & \alpha\nu^{-1}\sin\,(\alpha\nu y) \\ -\alpha^{-1}\nu\,\sin\,(\alpha\nu y) & \cos\,(\alpha\nu y) \end{bmatrix}. \tag{56}$$

Thus, the matrix of propagation through the layer interval $(x_l, x_l + h)$ is equal to $\mathbf{R}(h; \alpha; \omega)$ and depends on the thickness h and the dielectric parameter α (53) of the layer. So, for the matrix (17) of propagation over the two-layer period cell (6) we have, taking into account Eq. (14),

$$\mathbf{T}=\mathbf{R}(L_2;\alpha_2;\omega)\mathbf{R}(L_1;\alpha_1;\omega),\quad \alpha_{1,2}=\sqrt{\epsilon_{1,2}},\qquad (57)$$

and for the matrix (19) of propagation over the one-layer defect interval (7) we have

$$\mathbf{S}=\mathbf{R}(D;\alpha_3;\omega),\quad \alpha_3=\sqrt{\epsilon_3}.\qquad (58)$$

Using Eq. (56) in Eqs. (57) and (58), we obtain

$$t_{11}=\cos(\mu_1)\cos(\mu_2)-\frac{\alpha_2}{\alpha_1}\sin(\mu_1)\sin(\mu_2),$$

$$t_{21}=-\nu\left[\frac{1}{\alpha_1}\sin(\mu_1)\cos(\mu_2)+\frac{1}{\alpha_2}\cos(\mu_1)\sin(\mu_2)\right],$$

$$t_{12}=\frac{1}{\nu}[\alpha_1\sin(\mu_1)\cos(\mu_2)+\alpha_2\cos(\mu_1)\sin(\mu_2)],$$

$$t_{22}=\cos(\mu_1)\cos(\mu_2)-\frac{\alpha_1}{\alpha_2}\sin(\mu_1)\sin(\mu_2),\qquad (59)$$

and

$$s_{11}=\cos(\mu_3),$$

$$s_{21}=-\frac{\nu}{\alpha_3}\sin(\mu_3),$$

$$s_{12}=\frac{\alpha_3}{\nu}\sin(\mu_3),$$

$$s_{22}=\cos(\mu_3),\qquad (60)$$

where

$$\mu_i=\alpha_i L_i\nu=\alpha_i L_i\omega/c,\quad i=1,2,3\ \ (L_3=D).\qquad (61)$$

Thus, we have the following expressions for functions (45) and (46) engaged in Eq. (49) for the spectrum of the localized states:

$$\eta(\omega)=\cos(\mu_1)\cos(\mu_2)-p\sin(\mu_1)\sin(\mu_2),\qquad (62)$$

$$p=\frac{1}{2}\left(\frac{\alpha_2}{\alpha_1}+\frac{\alpha_1}{\alpha_2}\right)>1,\qquad (63)$$

$$\chi(\omega)=\tan(\mu_3)[q_1\sin(\mu_1)\cos(\mu_2)+q_2\cos(\mu_1)\sin(\mu_2)],\qquad (64)$$

$$q_i=\frac{1}{2}\left(\frac{\alpha_3}{\alpha_i}+\frac{\alpha_i}{\alpha_3}\right)>1,\quad i=1,2.\qquad (65)$$

Observe that the functions $\eta(\omega)$ and $\chi(\omega)$ in Eqs. (62), (63) and (64), (65) with (61) do not alter if parameters of the first and second substances are exchanged. Hence, we can assume with no loss of generality that

$$\alpha_2>\alpha_1.\qquad (66)$$

Note also that η and χ in Eqs. (62), (63) and (64), (65) with (61) can be represented as functions of the scaled spectral variable, $\mu=\alpha_0 L_0\omega/c$, to depend on the relative dielectric parameter, α_i/α_0 and relative thickness, L_i/L_0 of the layers, $i=1,2,3$, where α_0 and L_0 are parameters of one of them. This is a consequence of the general scaling property (8) of the spectral problem (3).

The wave function $\psi(x)$ for a spectral mode can be found explicitly on each period cell interval (x_n,x_n+L), $n=1,\pm2,\pm3,\ldots$, and on the defect interval (x_{-1},x_1). We can do that starting from the left end point x_n of the interval and using the propagation relation (11), (14) with the matrix (55), (56) in each homogeneous layer. The wave function at each point x_n, $n=\pm1,\pm2,\pm3,\ldots$, is determined by Eqs. (26), (18) or (35), (38) for propagating or localized modes, respectively.

V. ANALYSIS OF THE SPECTRUM

Representing functions (62) and (64) in Eq. (49) for the spectrum of the localized states in terms of the rescaled spectral variable

$$\mu=\alpha_1 L_1\omega/c,\qquad (67)$$

we have

$$\eta(\mu)=\cos(\mu)\cos(r\mu)-p\sin(\mu)\sin(r\mu),\qquad (68)$$

$$r=\frac{\alpha_2}{\alpha_1}\frac{L_2}{L_1},\qquad (69)$$

and

$$\chi(\mu)=\tan(v\mu)[q_1\sin(\mu)\cos(r\mu)+q_2\cos(\mu)\sin(r\mu)],\qquad (70)$$

$$v=\frac{\alpha_3}{\alpha_1}\frac{D}{L_1}.\qquad (71)$$

Let us firstly analyze inequality (51) for the gaps in the continuous spectrum, as they confine spectral values for possible localized states. We can represent the function $\eta(\mu)$ Eq. (68) in the phase-amplitude form:[18]

$$\eta(\mu)=A(\mu)\cos(\theta(\mu)),\qquad (72)$$

$$\theta(\mu)=r\mu+\phi(\mu),\qquad (73)$$

$$A(\mu)=\frac{\cos(\mu)}{\cos(\phi)},\qquad (74)$$

where $\theta(\mu)$ and $A(\mu)$ are the phase and the amplitude, respectively, and

$$\tan(\phi)=p\tan(\mu).\qquad (75)$$

The last equation can be solved for ϕ as

$$\phi(\mu)=\mu+\arctan\left(\frac{g\sin(2\mu)}{1-g\cos(2\mu)}\right),\qquad (76)$$

$$g=\frac{p-1}{p+1},\quad 0<g<1,\qquad (77)$$

so, A in Eq. (74) is non-negative and, using Eq. (75), we obtain

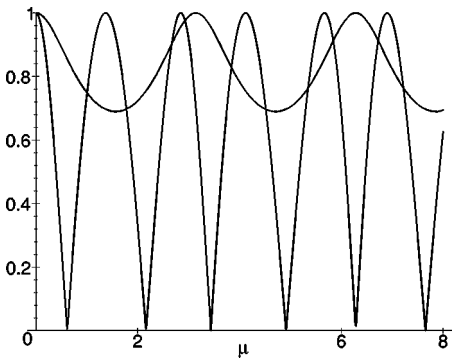

FIG. 1. Graphical representation of Eq. (80) for the edges of gaps in the continuous spectrum in terms of the scaled spectral variable, $\mu=\sqrt{\varepsilon_1}L_1\omega/c$.

$$A(\mu)=\sqrt{1+(p^2-1)\sin^2(\mu)}. \tag{78}$$

Using the phase-amplitude representation (72), the gap inequality (51) can be written as

$$|\cos\,(\theta(\mu))|>\frac{1}{A(\mu)}. \tag{79}$$

It defines the gaps (μ^l,μ^u) in terms of the rescaled spectral variable μ. The gap-edge points μ^l (lower edge) and μ^u (upper edge) satisfy the corresponding equation

$$|\cos\,(\theta(\mu))|=\frac{1}{A(\mu)}. \tag{80}$$

This equation is represented graphically in Fig. 1 at $\alpha_2/\alpha_1=2.5$ and $L_2/L_1=0.5$.

The amplitude function (78) oscillates between 1 and p,

$$1\leqslant A(\mu)\leqslant p. \tag{81}$$

Relations (75), (74), and (81) imply

$$\phi'(\mu)=\frac{p}{A^2(\mu)}\geqslant\frac{1}{p}>0, \tag{82}$$

so, the phase function $\theta(\mu)$ in Eq. (73) is monotonically increasing. In addition to that, using Eqs. (73), (82), and (78) one can show that

$$|\partial_\mu|\cos\,(\theta(\mu))||>\left|\partial_\mu\frac{1}{A(\mu)}\right| \quad \text{if} \quad |\cos\,(\theta(\mu))|=\frac{1}{A(\mu)}. \tag{83}$$

Due to Eqs. (81), (82), and (83), there is exactly one root of Eq. (80) contained in each interval of monotonicity of the function $|\cos\,(\theta(\mu))|$. So, we have the following inequalities for the edges μ^l and μ^u of each gap (μ^l,μ^u):

$$\mu_n^0<\mu_n^l<\bar{\mu}_n<\mu_n^u<\mu_{n+1}^0, \tag{84}$$

where $\bar{\mu}_n$ is one of points of the maximum of the $|\cos\,(\theta(\mu))|$,

$$\theta(\bar{\mu}_n)=n\pi, \quad n=1,2,3,\ldots, \tag{85}$$

and μ_n^0 and μ_{n+1}^0 are two adjacent to $\bar{\mu}_n$ zeroes of $|\cos\,(\theta(\mu))|$,

$$\theta(\mu_n^0)=\left(n-\frac{1}{2}\right)\pi, \quad n=1,2,3,\ldots\,. \tag{86}$$

The point $\bar{\mu}_n$ can be called a center of the nth gap (μ_n^l,μ_n^u).

Relations (84), (85), and (86) allow us to separate roots of Eq. (80) for the gap edges, as it is necessary for numerical computations. The roots $\bar{\mu}_n$ and μ_n^0 $(n=1,2,3,\ldots)$ of Eqs. (85) and (86) themselves can be located using the inequality following from Eqs. (73) and (76),

$$|\theta(\mu)-(r+1)\mu|<\pi/2. \tag{87}$$

According to Eqs. (73) and (76), the phase function,

$$\theta(\mu)=(r+1)\mu+\arctan\left(\frac{g\,\sin\,(2\mu)}{1-g\,\cos\,(2\mu)}\right) \tag{88}$$

exhibits additive symmetric modulations in μ with the period π. At the same time it is growing with μ at an average rate of $(r+1)$ which by itself would correspond to the left-hand side in Eq. (79) being periodic in μ with the period $\pi/(r+1)$. In the right-hand side in Eq. (79), the amplitude function (78) oscillates in μ with the period π. At $\mu=0$ both the left- and right-hand sides in Eq. (79) are equal to 1. Thus, if the ratio r (69) is rational, the periods $\pi/(r+1)$ and π become commensurate, then the gaps with such numbers n in Eq. (84) that

$$n=m(r+1), \quad m=1,2,3,\ldots, \tag{89}$$

will be closed. In general, the closer the center $\bar{\mu}_n$ of the nth gap [where $|\cos\,(\theta(\mu))|=1$; see Eq. (85)] is to a value $m\pi$, $m=1,2,3,\ldots$, [where $A(\mu)=1$; see Eq. (78)] the narrower the gap is. On the contrary, the closer the center $\bar{\mu}_n$ of the nth gap is to a value $(m-\frac{1}{2})\pi$, $m=1,2,3,\ldots$, [where both $1/A(\mu)$ and $\theta'(\mu)$ are minimal; see Eqs. (78), (73), and (82)] the wider the gap is. So, the gap width $(\mu_n^u-\mu_n^l)$ oscillates with the gap number n, while an average gap width does not decrease for higher n. (This is different from the situation with an analogous Schrödinger problem[16] where the gap width decreases to zero at higher gap numbers.)

One can see in Eqs. (84), (85), (86), and (88) that when r increases [due to increase of the dielectric contrast α_2/α_1 or of the thickness ratio L_2/L_1 for the two-layer medium; see Eq. (69)] then the edge values $\mu^{l,u}$ will decrease for all gaps. At the same time, the width of each gap will oscillate, starting from zero at $r=0$.

One may also see in Eqs. (79) and (78) with Eq. (63) that when the contrast $\alpha_2/\alpha_1>1$ increases, the ratio of an average gap width over an average band width also increases. At $\alpha_2/\alpha_1\to\infty$ all bands are closing, while at $\alpha_2/\alpha_1=1$ all gaps were closed.

The results of numerical calculations for the edge values $\mu^{l,u}$ for the first five gaps at varying values of α_2/α_1 or L_2/L_1 are shown with solid lines in Figs. 2 and 3.

Let us now turn to Eq. (49) with Eqs. (68) and (70) for the spectral values μ^* for localized states. That equation is represented graphically in Fig. 4 at $\alpha_2/\alpha_1=2.5$, $L_2/L_1=0.5$, $\alpha_3/\alpha_1=2$, and $D/L_1=1.5$.

The first factor in $\chi(\mu)$ in Eq. (70) changes monotonically from 0 to $\pm\infty$ on each interval $[m\pi/v,(m\pm1/2)\pi/v]$, $m=1,2,3,\ldots$, while $\eta(\mu)$ in Eq. (68) is bounded. Hence,

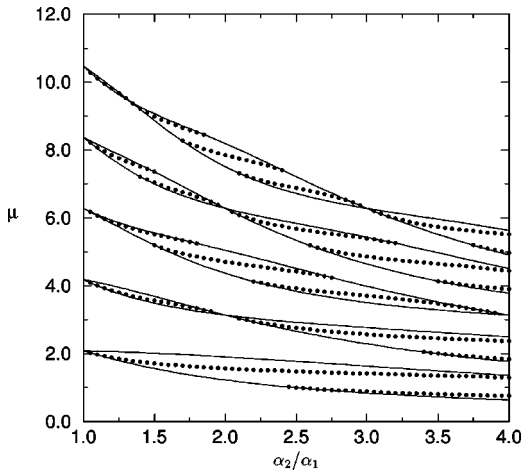

FIG. 2. Scaled spectral value, $\mu=\sqrt{\varepsilon_1}L_1\omega/c$ for the gap edges (solid lines) and for the localized states (dots) at varying dielectric contrast, $\alpha_2/\alpha_1=\sqrt{\varepsilon_2/\varepsilon_1}$ between two layers in the period cell with the thickness ratio $L_2/L_1=0.5$.

there will be a solution μ^* of Eq. (49) in one of the two such intervals adjacent to each of zero points μ' of the first factor in $\chi(\mu)$ in Eq. (70),

$$\mu'_m=m\pi/v, \quad m=1,2,3,\ldots, \tag{90}$$

if the point μ' is located in a gap (μ_n^l,μ_n^u) [where $|\eta(\mu)|>1$, see Eq. (51)]:

$$\mu^*\in(\mu'_m,\mu'_m+\sigma\pi/2v) \quad \text{for} \quad \mu'_m\in(\mu_n^l,\mu_n^u), \tag{91}$$

$$\sigma=+1 \quad \text{or} \quad \sigma=-1.$$

In addition, the second factor in $\chi(\mu)$ in Eq. (70) has zeroes and changes sign at points μ'' where

$$\tan(r\mu'')=-u\tan(\mu'') \tag{92}$$

with

$$u=q_1/q_2. \tag{93}$$

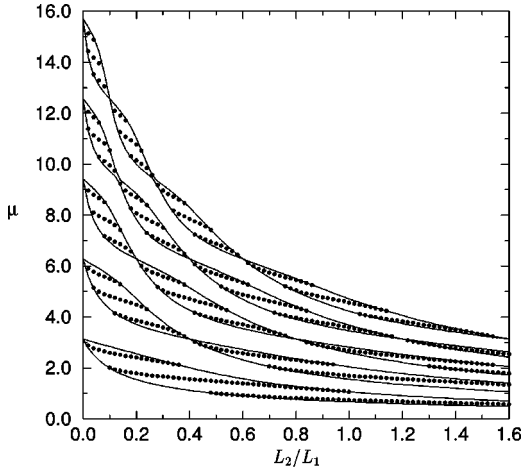

FIG. 3. Scaled spectral value, $\mu=\sqrt{\varepsilon_1}L_1\omega/c$ for the gap edges (solid lines) and for the localized states (dots) at varying thickness ratio L_2/L_1 between two layers in the period cell with the dielectric contrast $\alpha_2/\alpha_1=2.5$.

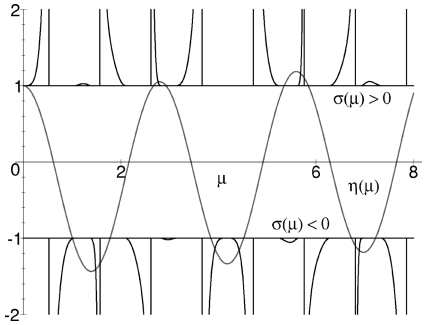

FIG. 4. Graphical representation of Eq. (49) for the scaled spectral value $\mu=\sqrt{\varepsilon_1}L_1\omega/c$ for localized states; $\sigma(\mu)=\text{sgn}\,(\chi)\sqrt{\chi^2+1}$.

There should be one such point μ'' next to the center $\overline{\mu}$ of each gap because

$$\tan(r\overline{\mu})=-p\,\tan(\overline{\mu}), \tag{94}$$

due to Eqs. (85), (73), and (75). Moreover, we can show that each such point μ'' is located in a gap. Indeed, using Eqs. (68) and (92) we obtain

$$\eta^2(\mu'')=\frac{(1+puz)^2}{(1+z)(1+u^2z)}, \quad z=\tan^2(\mu'')>0. \tag{95}$$

It is easy to show that the quotient u [see Eqs. (93) and (65)] is confined between values α_2/α_1 and α_1/α_2 at any values of the parameters α_i, $i=1,2,3$, so that $u+1/u<2p$ [see Eq. (63)]. This provides $\eta^2(\mu'')>1$ in Eq. (95), so, μ'' satisfies the gap inequality (51). Thus, there is one point μ'' in each gap (μ^l,μ^u):

$$\mu''_n\in(\mu_n^l,\mu_n^u), \quad n=1,2,3,\ldots. \tag{96}$$

Due to that, the number of solutions μ^* of Eq. (49) located in each gap is one more than the number of points μ' present in that gap. Indeed, if there are points μ' in a gap, then the change of sign of $\chi(\mu)$ over the point μ'' yields the presence of two solutions μ^* next to one point μ' (the closest to μ''), one solution μ^* on each side of the point μ'; that is described by both $\sigma=+1$ and $\sigma=-1$ in Eq. (91). If there are no points μ' in a gap, there still is one solution μ^* in it, because $\chi(\mu)$ has zero at the point μ''. So, there is at least one spectral value μ^* for a localized state in each gap.

One can see in Eq. (91) with Eq. (90) that when v increases [due to increase of the defect-medium dielectric contrast α_3/α_1 or of the relative thickness D/L_1 of the defect layer, see Eq. (71)] then each spectral value μ^* will arise at the upper edge μ^u of a gap, decrease, and vanish at the lower edge μ^l of the gap, while an average number of the spectral values μ^* in each gap is increasing.

Results of numerical calculations for the spectral values μ^* for localized states in the first five gaps at varying values of α_3/α_1 or D/L_1 are shown in Figs. 5 and 6 at $\alpha_2/\alpha_1=2.5$ and $L_2/L_1=0.5$.

The rate of localization (36) for a defect-induced state (35) with a spectral value μ^* is equal to $\tau(\mu^*)$ where the function

$$\tau(\mu)=|\eta|+\sqrt{\eta^2-1}, \tag{97}$$

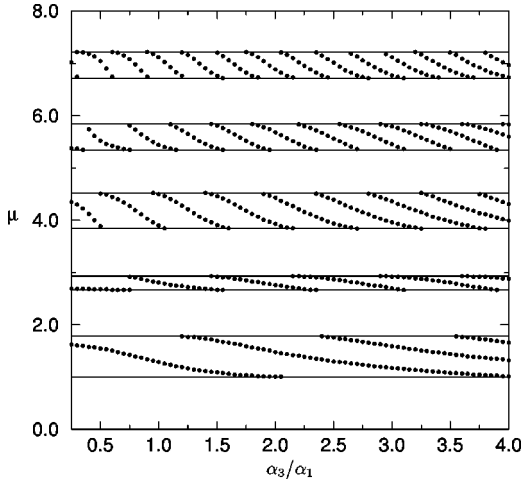

FIG. 5. Scaled spectral value, $\mu=\sqrt{\varepsilon_1}L_1\omega/c$ for the localized states at varying defect-medium dielectric contrast, $\alpha_3/\alpha_1=\sqrt{\varepsilon_3/\varepsilon_1}$ for the defect relative thickness $D/L_1=1.5$.

[see Eq. (50)] depends on parameters α_2/α_1 and L_2/L_1 of the periodic medium [see Eq. (68) with Eqs. (63) and (69)] and does not depend on the parameters of the defect. The graph of the function $\tau(\mu)$ is shown in Fig. 7 (with the vertical μ axis) at $\alpha_2/\alpha_1=2.5$ and $L_2/L_1=0.5$.

One can see that when the spectral value μ^* spans a gap (with a number n) following variations of the parameters of the defect, the multiplicative rate $\tau(\mu^*)$ of localization increases from 1 at one edge of the gap up to a maximum in the middle of the gap and then decreases to 1 at the other edge of the gap. According to Eqs. (97), (72), and (81), the highest possible value of the maximum of $\tau(\mu^*)$ in a gap at a given value of α_2/α_1 is

$$\tau_{\max}=p+\sqrt{p^2-1}, \tag{98}$$

which is greater for higher values of $\alpha_2/\alpha_1>1$ [see Eq. (63)]; this value may be actually reached by tuning the ratio L_2/L_1 in such a way that the center $\overline{\mu_n}$ of the gap [see Eq. (85)] coincides with a point $(m-\frac{1}{2})\pi$ of maximum of the function $A(\mu)$ in Eq. (78).

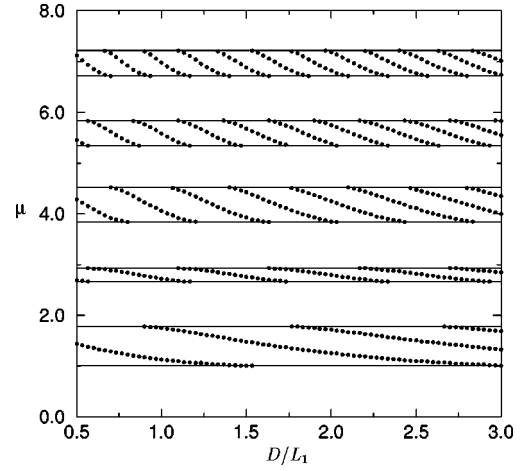

FIG. 6. Scaled spectral value, $\mu=\sqrt{\varepsilon_1}L_1\omega/c$ for the localized states at varying relative thickness D/L_1 of the defect layer with the dielectric contrast $\alpha_3/\alpha_1=2$.

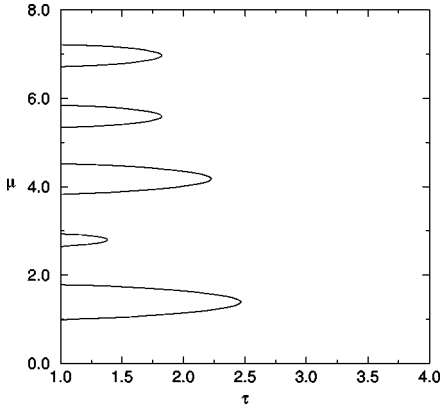

FIG. 7. Multiplicative rate τ of localization for a defect-induced state versus its scaled spectral value $\mu=\sqrt{\varepsilon_1}L_1\omega/c$ at the dielectric contrast $\alpha_2/\alpha_1=2.5$, and the thickness ratio $L_2/L_1=0.5$ in the two-layer periodic medium.

Concerning variations of parameters of the periodic medium, one can see in Eq. (91) with Eq. (90) that when α_2/α_1 or L_2/L_1 increases each spectral value μ^* will arise at the lower edge μ^l and vanish at the upper edge μ^u of a gap due to decrease of the edge values for all gaps as discussed above. The results of numerical calculations for the spectral values μ^* for localized states in the first five gaps at varying values of α_2/α_1 or L_2/L_1 are shown with dots in Figs. 2 and 3 at $\alpha_3/\alpha_1=2.0$ and $D/L_1=1.5$. We observe that the values μ^* decrease with the increase of α_2/α_1 or L_2/L_1.

VI. CONCLUSIONS

We obtained the following general results for an arbitrary 1D periodic dielectric system with an embedded defect: (i) the frequency spectrum of electromagnetic modes consists of a continuous set and a discrete set; (ii) the continuous spectrum coincides with the entire spectrum for the same periodic medium without a defect; (iii) the discrete spectrum is located in the gaps of the continuous spectrum and corresponds to localized waves that decay exponentially away from the defect; (iv) the rate of localization of a defect-induced mode depends on the configuration of the defect only through the mode frequency; (v) the localized wave delocalizes when its frequency approaches the gap edges.

These results agree with the general analysis[19] of the spectral problem for periodic 1D [as in the left-hand side of Eq. (3)] and 3D Maxwell operators with perturbations. It was proven there that the continuous spectrum is stable under a local perturbation of the periodic operator. It was also shown that discrete eigenvalues can be induced in the gaps of the spectrum of the unperturbed operator and correspond to exponentially localized eigenmodes.

For a particular situation of a one-layer defect in a two-layer periodic medium we carry out complete analysis of the gaps in the continuous spectrum and of the existence of localized modes and of their dependence on parameters of the system: (i) we show that an average gap width does not decrease for higher gap numbers; (ii) we prove analytically that there always is at least one discrete spectral value in each gap of the continuous spectrum; (iii) we show analytically and numerically that when the dielectric contrast be-

tween the defect and the periodic medium or the relative thickness of the defect layer increases then the discrete spectral values arise at the top of a gap, decrease, and vanish at the bottom of the gap, while an average number of the spectral values in each gap increases; (iv) we observe that the rate of localization of a defect-induced mode is greater for frequencies in the middle of the gap and for wider gaps; (v) we obtain a simple formula for the maximal possible rate of localization and show that it depends only on the dielectric contrast between two layers in the cell of the periodic medium and increases with the contrast.

These results are consistent with the general operator analysis[20] for the number and behavior of the defect-induced eigenvalues in a gap. The decrease of the discrete eigenvalues is related to the decrease of the perturbed Maxwell operator with the increase of the dielectric constant of the defect. The localization of a mode induced by a local defect is related to the exponential decay of the Green's function for the periodic Maxwell operator with the decay rate depending on the dielectric contrast in the periodic medium. The presence of a defect eigenvalue in every gap at any values of parameters of the defect is probably the only artifact of the 1D system. For a 3D system there is a threshold[20] for the strength of a local defect for localized eigenmodes with frequencies in a gap to arise.

ACKNOWLEDGMENTS

We thank Professor S. Molchanov for useful discussions. The work of A.F. and V.G. was sponsored by the Air Force Office of Scientific Research, Air Force Materials Command, USAF, under Grant No. F49620-94-1-0172DEF and F49620-97-1-0019.

[1] *Photonic Band Gaps and Localization*, edited by C. M. Soukoulis (Plenum, New York, 1993).
[2] *Development and Application of Materials Exhibiting Photonic Band Gaps*, special issue of J. Opt. Soc. Am. B **10**, 280 (1993).
[3] *Photonic Band Structures*, special issue of J. Mod. Opt. **41**, 171 (1994).
[4] *Photonic Band Gap Materials*, edited by C. M. Soukoulis (Kluwer Academic, Dordrecht, 1996).
[5] *Microcavities and Photonic Bandgaps*, edited by J. Rarity and C. Weisbuch (Kluwer Academic, Dordrecht, 1996).
[6] E. Yablonovitch, in Ref. 3, pp. 173–194.
[7] J. W. Haus, in Ref. 3, pp. 195–207.
[8] E. Yablonovitch, T. J. Gmitter, R. D. Meade, A. M. Rappe, K. D. Brommer, and J. D. Joannopoulos, Phys. Rev. Lett. **67**, 3380 (1991).
[9] D. R. Smith, R. Dalichaouch, N. Kroll, S. Schultz, S. L. McCall, and P. M. Platzman, in Ref. 2, pp. 314–322.
[10] S.Schultz and D. R. Smith, in Ref. 1, pp. 305–316.
[11] D. R. Smith, S. Schultz, S. L. McCall, and P. M. Platzman, in Ref. 3, pp. 395–404.
[12] R. D. Meade, K. D. Brommer, A. M. Rappe, and J. D. Joannopoulos, Phys. Rev. B **44**, 13 772 (1991).
[13] A. A. Maradudin and A. R. McGurn, in Ref. 1, pp. 247–268.
[14] R. D. Meade, A. M. Rappe, K. D. Brommer, J. D. Joannopoulos, and O. L. Alerhand, Phys. Rev. B **48**, 8434 (1993).
[15] K. Busch, C. T. Chan, and C. M. Soukoulis, in Ref. 4, pp. 465–485.
[16] M. Reed and B. Simon, *Methods of Modern Mathematical Physics* (Academic Press, New York, 1978), Vol. IV.
[17] A. Figotin and P. Kuchment, SIAM (Soc. Ind. Appl. Math.) J. Appl. Math. **56**, 68 (1996).
[18] A. Figotin and Yu. Godin, J. Comput. Phys. **136**, 585 (1997).
[19] A. Figotin and A. Klein, J. Stat. Phys. **86**, 165 (1997).
[20] A. Figotin and A. Klein, SIAM J. Appl. Math. (to be published).